



Technological University Dublin
ARROW@TU Dublin

Articles

School of Electrical and Electronic Engineering

2018

High Sensitivity Optical Fiber Sensors for Simultaneous Measurement of Methanol and Ethanol

Dejun Liu

Technological University Dublin, d13127141@mydit.ie

Rahul Kumarb

Northumbria University, Newcastle Upon Tyne

Fangfang Wei

Technological University Dublin


Wei Han

Technological University Dublin

Arun Kumar Mallik

Technological University Dublin

Follow this and additional works at: <https://arrow.tudublin.ie/engscheceart>

 Part of the [Engineering Commons](#)
See next page for additional authors

Recommended Citation

Wu, Q. et al. (2018) High Sensitivity Optical Fiber Sensors for Simultaneous Measurement of Methanol and Ethanol, *Sensors and Actuators B: Chemical* Vol. 271, 15 October 2018, Pages 1-8. doi.org/10.1016/j.snb.2018.05.106

This Article is brought to you for free and open access by the School of Electrical and Electronic Engineering at ARROW@TU Dublin. It has been accepted for inclusion in Articles by an authorized administrator of ARROW@TU Dublin. For more information, please contact yvonne.desmond@tudublin.ie, arrow.admin@tudublin.ie, brian.widdis@tudublin.ie.



This work is licensed under a [Creative Commons Attribution-NonCommercial-Share Alike 3.0 License](#)



Authors

Dejun Liu, Rahul Kumarb, Fangfang Wei, Wei Han, Arun Kumar Mallik, Jinhui Yuanc, Shengpeng Wan, Xingdao He, Zhe Kange, Feng Li, Chongxiu Yu, Gerald Farrell, Yuliya Semenova, and Qiang Wu

High sensitivity optical fiber sensors for simultaneous measurement of methanol and ethanol

Dejun Liu^{a,b}, Rahul Kumar^b, Fangfang Wei^a, Wei Han^a, Arun Kumar Mallik^a, Jinhui Yuan^c, Shengpeng Wan^d, Xingdao He^d, Zhe Kang^e, Feng Li^e, Chongxiu Yu^c, Gerald Farrell^a, Yuliya Semenova^a and Qiang Wu^{b,*}

^aPhotonics Research Centre, Dublin Institute of Technology, Kevin Street, Dublin 8, Ireland

^bDepartment of Mathematics, Physics and Electrical Engineering, Northumbria University, Newcastle Upon Tyne, NE1 8ST, United Kingdom

^cState Key Laboratory of Information Photonics and Optical Communications, Beijing University of Posts and Telecommunications, Beijing 100876, China

^dJiangxi Engineering Laboratory for Optoelectronics Testing Technology, Nanchang Hangkong University, Nanchang 330063, China

^ePhotonics Research Centre, Department of Electronic and Information Engineering, The Hong Kong Polytechnic University, Hong Kong

*Corresponding author: qiang.wu@northumbria.ac.uk

Abstract

High sensitivity volatile organic compounds (VOCs) sensors based on a tapered small core single mode fiber (TSCSMF) and a microfiber coupler (MFC) are reported. The TSCSMF had a waist diameter of $\sim 5.1 \mu\text{m}$ and the MFC had a waist diameter of $\sim 1.9 \mu\text{m}$ each and both were fabricated using a customized microheater brushing technique. Silica based materials containing immobilized Nile red prepared by sol-gel method with two different recipes (recipe I and recipe II) are investigated. Initially recipe I based coating materials were applied to the surfaces of the TSCSMF and MFC. The experimental results show that the sensor based on an MFC shows much better sensitivities of -0.130 nm/ppm and -0.036 nm/ppm to ethanol and methanol than those of the TSCSMF based sensor. The corresponding minimum detectable concentration change of the MFC based sensor are calculated to be $\sim 77 \text{ ppb}$ and $\sim 281 \text{ ppb}$ to ethanol and methanol respectively. Both sensors are demonstrated fast response times of less than 5 minutes, while the recovery times varied from 7 minutes to 12 minutes. In addition, another TSCSMF based sample ($\sim 7.0 \mu\text{m}$) coated with a mixed layer of sol silica and Nile red prepared by recipe II was fabricated to achieve simultaneous measurement of ethanol and methanol, employing a second-order matrix approach.

Keywords: Volatile organic compounds, optical fiber sensor, tapered fiber, sol-gel silica, Nile red

1. Introduction

Volatile organic compounds (VOCs) are the major pollutants for indoor environments, as a result of their presence in many household products (e.g. paints, wax and furniture) and combustion processes (e.g. heating and smoking). Inhaling excess VOCs and their degradation products may cause respiratory system damage or even cancer [1-2]. Studies show that VOCs may be also related to global warming, stratospheric ozone depletion and photochemical ozone [3]. The growing awareness of the negative impact of VOCs on both human health and the global environment has been attracting increasing efforts to improve the detection, monitoring and analysis of VOCs. So far, a number of sensing techniques have been proposed to monitor the concentration of VOCs, such as semi-conductor metal oxides detectors [4], surface acoustic wave methods [5], chemiresistors [6], colorimetric sensors [7], infrared attenuated total reflection (IR-ATR) spectroscopy [8] and fiber optics sensors [9-10]. Among these techniques, fiber optic sensors have been attracting significant attention due to their well-known advantages, such as compact size, real-time operation, immunity to electromagnetic interference and remote sensing capabilities.

Deposition of additional materials on the fiber surface is usually required to implement an optical fiber based VOCs sensor. To date, a range of sensitive materials for various VOCs have been proposed, including hydrophobic ethylene/propylene (60/40) co-polymer [8], chemical dyes with solvatochromic properties [9], semiconductor metal oxides (TiO_2 , ZnO , ITO) [11-13], zeolite thin film [14], polymethyl methacrylate (PMMA) film [15], poly (dimethylsiloxane) (PDMS) film [16] vapo-chromic materials [17], metal based nanomaterials [18], and p-sulphanatocalix arene [19]. Among these, ethylene/propylene (60/40) co-polymer, solvatochromic

dye materials, and semiconductor metal oxides have been found to possess relatively high sensitivities to VOCs (providing detection resolution in the level of ppb) and as a result semiconductor metal oxides have been widely used in commercial chemical vapor sensors. However, a significant disadvantage of these materials is that while they normally operate well at a high temperature (200-500 °C) they display a very limited gas sensitivity at room temperature (usually with a detection resolution of tens or hundreds of ppm [11-12]). As an alternative recently, Khan et. al. [9] have proposed a highly sensitive VOCs sensor based on a side-polished single-mode fiber with a coating layer incorporating a solvatochromic dye material (Nile red) with N, N-dimethylacetamide (DMAC) and polyvinylpyrrolidone (PVP). However the sensor proposed by Khan et al suffer from the disadvantage of a narrow measurement range (less than 9 ppb), compounded by a complex fabrication process and demodulation scheme.

Porous silica prepared by the sol-gel method offers chemical and thermal stability, an inert nature and transparency over a wide range of wavelengths, which has been widely used in optical fiber based chemical sensors either as assistant materials for the purpose of immobilization of specific sensitive materials [20] or as a chemically sensitive material in itself [21-22]. In addition, the textural properties such as the pore size, pore ratio, refractive index and even morphology of porous silica can be tuned by customizing a wide range of preparation parameters including water/precursor/solvent molar ratio, pH and temperature during both the fabrication and the subsequent drying process [23-24]. To take full advantage of porous silica materials and the highly sensitive dye materials (Nile red) for sensing VOCs, we propose here a coating mixture of Nile red immobilized sol-gel silica suitable for VOCs detection.

Previously, we have demonstrated that both a tapered small core single mode fiber (TSCSMF) and a microfiber coupler (MFC) are highly sensitive to surrounding refractive index change and have been developed as high sensitivity ammonia sensors [21, 25-26]. In this work we report high sensitivity VOCs sensors based on both TSCSMF and MFC structures coated with a layer consisting of a mixture of Nile red and sol-gel silica. Besides we also demonstrate simultaneous measurement of methanol and ethanol concentrations in air by using two TSCSMF based sensors functionalized with different coating layers based on different recipes.

2. Theory and operating principle of the sensors

2.1. Operation principle for the TSCSMF and MFC

The TSCSMF is based on the coupling of multiple modes within a single fiber structure while in the MFC, the coupling of modes occurs between two individual fibers, which results in the different directions for the spectral shifts induced by the same environmental changes. Specifically, in our experiment, a red shift and a blue shift in the transmission spectra are observed with the increase of gas concentrations for the TSCSMF and MFC fiber sensors, respectively. The detailed operation principle of TSCSMF and MFC could be found in the previous reports, which is not listed here for the sake of brevity [21, 25-28].

2.2. Operating principle for Nile red

Nile red has been widely used as a solvent polarity indicator and for the measurement of solvent strength [29-30]. It is a dye material with positive solvatochromism properties, which indicates that a molecule in the first excited state is better stabilized by solvation than a molecule in the ground state, with increasing solvent polarity. The strength of intermolecular solute/solvent interactions and the dipole moment in the ground state and the excited state are dependent on the chemical structure and physical properties of the solute/solvent molecules [29]. In our experiment, when Nile red comes into contact with VOCs, the dipole moment changes from its ground state to an excited state due to the changed charge transfer between the donor (diethyl amino) and acceptor (carbonyl oxygen) moieties of Nile red. As a consequence, the energy band gap between the ground and the first excited state changes, further resulting in a change in the relative permittivity of the constituent molecules and hence a change in the refractive index of the dye material [31]. For use within a sensor, small changes in refractive index of the coating layer can be monitored by the tapered fiber structures used.

3. Experiments

3.1 Nile red immobilized sol-gel silica fabrication

The solution mixture of Nile red and sol-gel silica used for the coating was prepared as follows: (1) 10 ml of hydrolyzing tetraethylorthosilicate (TEOS) was mixed with 5 ml of ethanol for 20 minutes using magnetic

stirring at room temperature; (2) 1 ml 0.1 mol/L HCl solution was added into the mixture followed by further stirring for a certain amount of time, that is 40 minutes to produce recipe I and 120 minutes to produce recipe II; (3) 10 mg of Nile red was mixed with 6 ml of the sol solution obtained in step (2) under stirring for one more hour, after which the final sol solution was ready for the coating process. Due to the sol-gel process within the solution, a different stirring time results in different solution viscosity and hence a different refractive index, texture properties, coating thickness and a different Nile red concentration.

3.2 TSCSMF/ MFC fiber structures fabrication and dip coating process

In our experiment, two different fiber structures based on a TSCSMF and a MFC were fabricated by a customized microheater brushing technique; the detailed fabrication process can be found in [25-26]. Figure 1a and b illustrate the schematic diagrams of the proposed TSCSMF and MFC structures.

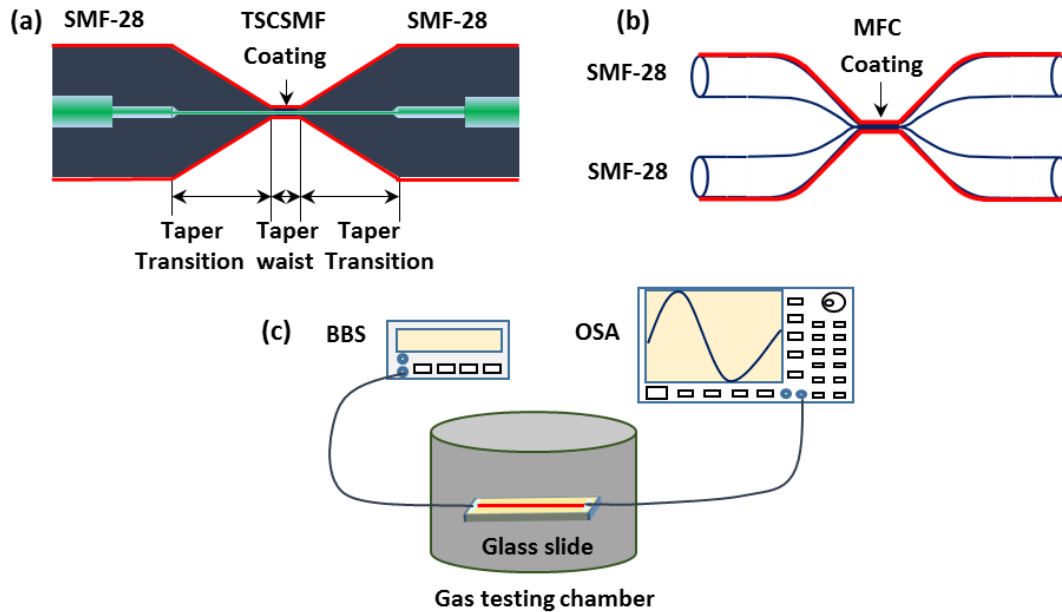


Fig. 1. Schematic diagram of: (a) TSCSMF, (b) MFC and (c) experimental setup for VOCs sensing.

A thin layer which has Nile red immobilized within silica gel (recipe I) was coated on the tapered fiber surface by a dip coating method, where a motor controlled translation stage was employed to pass a drop of the coating solution through each tapered fiber structure sample. A single pass coating cycle is defined as a one-pass coating. By repeating the one-pass coating process, different silica coating thicknesses can be realized. It should be noted that after each pass, the coating was left to dry for 6 minutes before the next coating layer was applied. After a repeating the one-pass dip coating process a number of times, the functionalized fiber sensor was cured at room temperature for three days before use.

3.3 Experimental setup for VOCs sensing

Figure 1c shows a schematic diagram of the experimental setup for VOCs sensing. Light from a broadband light source is launched into the fiber sensor structure and the transmitted light is measured by an optical spectrum analyzer (OSA). In order to realize different VOCs concentrations, different volumes of VOCs liquids (ethanol/methanol) were introduced into the gas testing cylindrical chamber (which has a diameter of 23 mm and a height of 11.5 mm) using a micro-syringe. The VOCs liquids evaporate naturally within the chamber, generating VOCs gas vapors with predictable concentrations which can be calculated according to a specific VOC mole ratio to air in the chamber. When the gas vapor is absorbed by the coating layer, the physical properties (refractive index and thickness) of the coating materials change, resulting in the variation of the measured spectral response of the sensor at different gas concentrations. Once the spectrum variation is calibrated, the concentration of the VOC can be determined. In the experiments, all tests were conducted at room temperature.

4. Results and discussion

4.1 Scanning electron microscope (SEM) and Energy-dispersive X-ray spectroscopy (EDS) analysis

Figure 2a illustrates an SEM image of the functionalized TSCSMF. As one can see from the figure, some small particles are attached to the fiber surface. These particles are clusters of undissolved Nile red ($C_{20}H_{18}N_2O_2$) which is confirmed by the EDS analysis on both a particle and smooth surface where increased carbon atoms in weight of 21.8% are detected on the particle compared to that of 10.18% on the smooth fiber surface. A very small amount of copper and zinc atoms were also detected due to the use of a copper sheet to support the fiber. SEM images of an MFC sample after its coating are presented in Fig. 2b and c, showing similar coating features for the TSCSMF. The measure diameters of the TSCSMF and MFC are found to be $\sim 5.1 \mu\text{m}$ and $\sim 1.9 \mu\text{m}$ (for each tapered SMF), respectively.

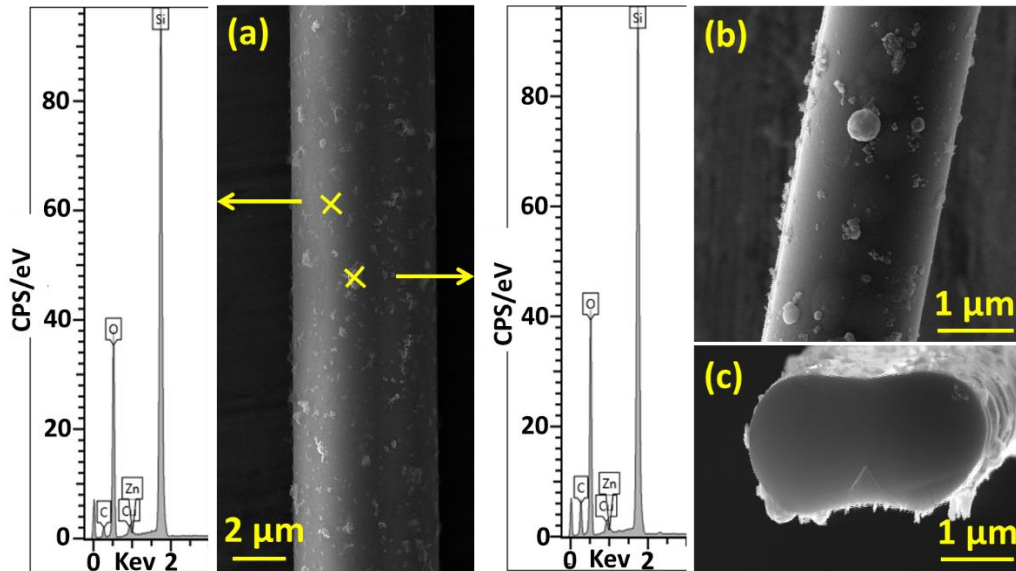


Fig. 2. SEM images of (a) TSCSMF, (b) MFC and (c) the cross section of MFC after coating with Nile red immobilized sol-gel silica ([recipe I](#)). EDS results on the coating surface of TSCSMF sample are also shown in (a).

4.2 Spectral response to VOCs for the sensors based on the TSCSMF and MFC.

Examples of the measured spectral responses for the 8-pass coating TSCSMF sensor and the 4-pass coating MFC sensor exposed to different ethanol concentrations are shown in Fig. 3a and b. Different numbers of coating passes were chosen for the different sensor types since from previous experience it was found that a thicker coating would result in a higher sensitivity [21], but in practice it was found that the MFC is too fragile to be coated more than 8 times due to its smaller tapered waist diameter compared to the SCSMF. It is also noted that even with the same number of coating passes, the actual coating thickness achieved can be different because of variations in the tapered diameter [32]. As can be seen from Fig. 3a, the spectral dip wavelength of the TSCSMF based sensor shifts toward a longer wavelength (red shift) as the VOC's concentration increases. In contrast, a blue shift is observed for the MFC based sensor as shown in Fig. 3b.

The spectral responses for the measurement of the other VOC used, methanol, are not shown here for the sake of brevity since they have similar spectral responses but different wavelength shift values. Figure 3c and d summarize the measured wavelength shifts at different concentrations of ethanol and methanol. In the figures, we define a red shift as a positive wavelength shift while the blue shift as a negative wavelength shift. The wavelength shifts versus gases concentrations show good linearity for both sensors, but the sensor based on an MFC exhibits better sensitivities of -0.130 nm/ppm and -0.036 nm/ppm to ethanol and methanol respectively, compared to those of 0.018 nm/ppm and 0.005 nm/ppm for the TSCSMF based sensor. This is reasonable since that smaller taper waist diameter of the MFC leads to an increase in the portion of the evanescent field exposed to the surrounding environment and hence results in a higher sensitivity for the sensor. Furthermore the sensor's sensitivity S is defined as $S = \Delta\lambda/C$, where C is the VOCs concentration and $\Delta\lambda$ represents the corresponding spectral wavelength shift for different VOCs concentrations. Assuming an OSA has a wavelength resolution of 0.01 nm , the minimum detectable concentration change of the MFC for ethanol and methanol are about 77 ppb and 281 ppb , which is over one magnitude higher than the previous reports in which the minimum detectable concentration change at a level of ppm were achieved [10, 14-17].

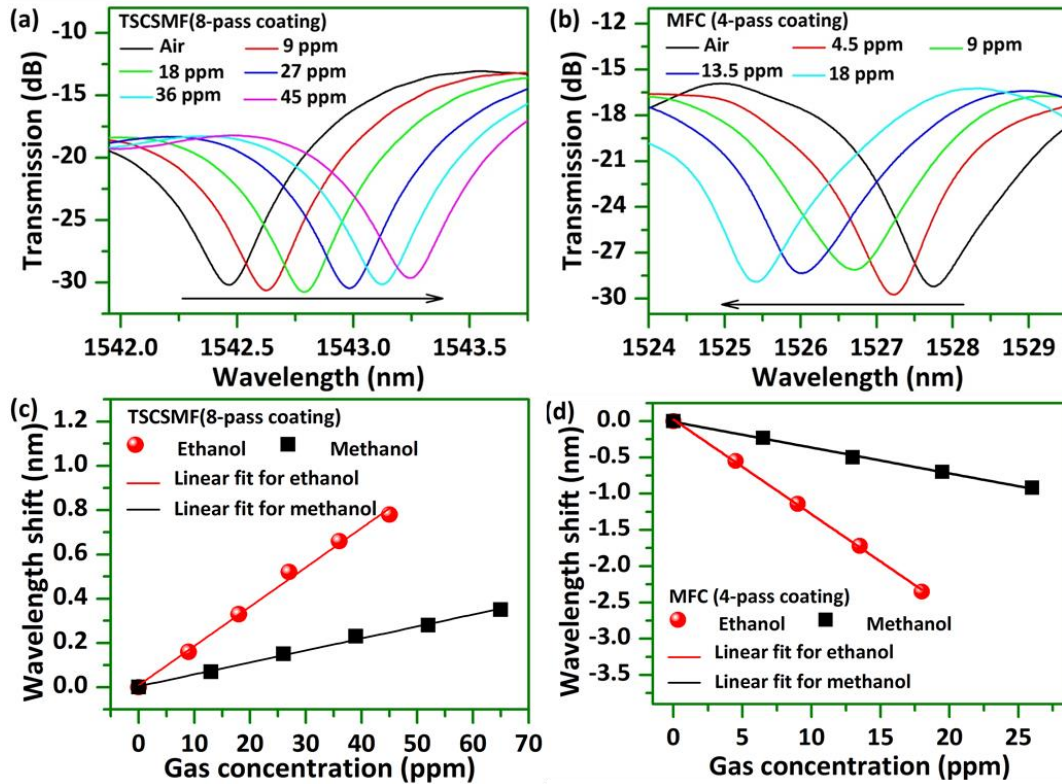


Fig. 3. Normalized measured spectral response at different concentrations of ethanol for (a) TSCSMF with 8-pass coating and (b) MFC with 4-pass coating; Measured corresponding wavelength shifts for different VOCs and concentrations for (c) TSCSMF with 8-pass coating and (d) MFC with 4-pass coating.

The response and recovery times of sensors to both ethanol and methanol are also investigated at selected gas concentrations and examples are illustrated in Fig. 4. The response time is defined as the time during which the sensor's response reaches 90% of its full response in terms of wavelength shift and the recovery time as the time it takes for it to fall to 10% of the full response. The sensor based on a TSCSMF (Fig. 4a) shows a faster response time of 2 minutes and a recovery time of 8 minutes. For the measurement of the response of the TSCSMF to ethanol, it is apparent that the response overshoots initially (data points circled with a purple dashed line). We believe this can be attributed to the fast contact and reaction between the sensor head and the gas under test whose concentration is initially uneven throughout the chamber due to combined effects of spatial variations in liquid evaporation and gas diffusion, after the VOCs liquid drops are introduced into the chamber. To achieve a more stable change of gas concentration surrounding the sensor head, in tests for the MFC based sensor, a flat steel sheet was placed between the sensor head and the liquid drop point in the chamber to avoid an overly fast interaction. As shown in Fig. 4b, no evidence of overshoot is observed, the MFC based sensor shows faster response of less than 5 minutes to both ethanol and methanol, but a longer recovery time of about 12 minutes is required for methanol compared with that for ethanol. It should be noted that the actual sensor response times are likely to be shorter than our measured results, due to the time taken by the liquids to evaporate within the chamber and for the VOCs to be evacuated from the volume space of the chamber.

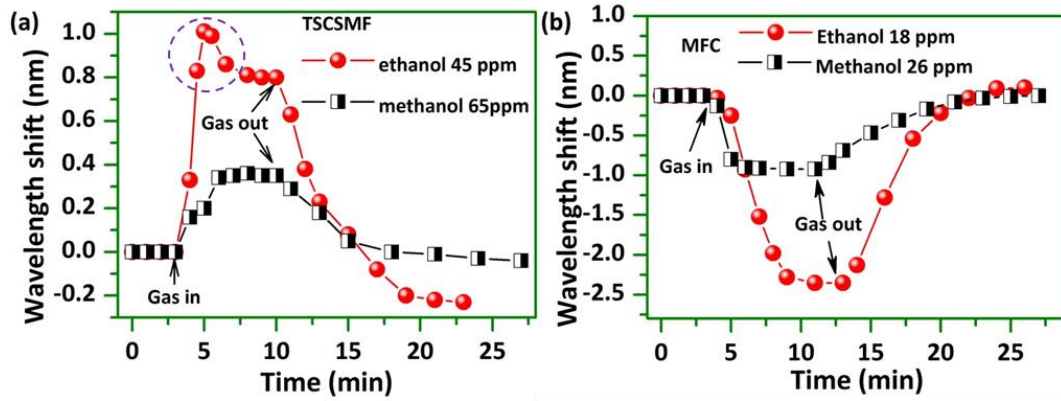


Fig. 4. Spectral response and recovery of (a) TSCSMF based sensor with 8-pass coating and (b) MFC based sensor with 4-pass coating to ethanol and methanol at selected gas concentrations.

4.3 Measurement Repeatability

Selected ethanol concentrations were chosen to perform the repeatability tests for both sensors and the experimental results are shown in Fig. 5. The corresponding dip wavelength shifts are summarized in Table 1 which shows a very minor wavelength shift variation recorded for three tests carried at fixed time intervals, demonstrating that both sensors show good repeatability. It is noted that after each round of tests, the wavelength dip of both sensors does not return to the original wavelength, which is possibly due to the reaction between the VOCs and coating materials, resulting in changes in the coating materials. However, the sensors for each test round do have similar relative wavelength shifts, following the introduction of the VOCs. This is subject of further investigation at present.

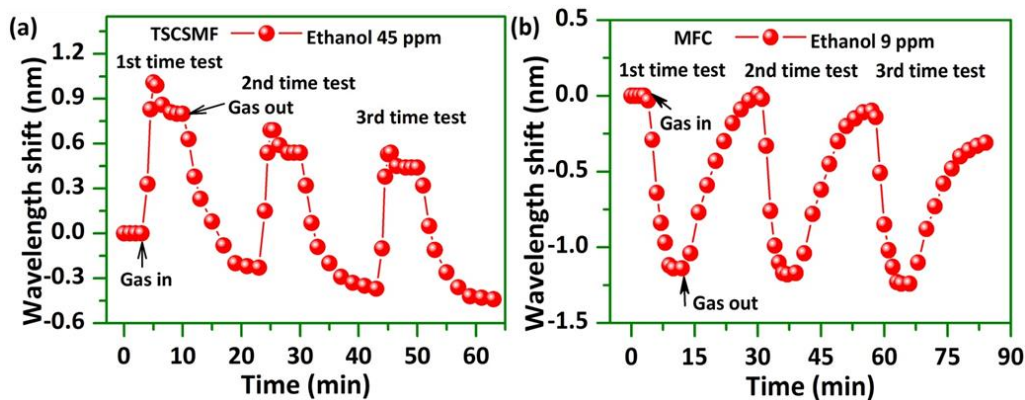


Fig. 5. Sensors' response and recovery illustrating reversibility and reproducibility of measurements for both sensors at selected ethanol concentrations of 45 ppm and 9 ppm: (a) TSCSMF; (b) MFC.

Table 1. Spectral dips wavelength shifts for the TSCSMF and MFC based sensors for a series of repeat tests at selected ethanol concentrations.

	1st test (nm)	2nd test (nm)	3rd test (nm)
TSCSMF	0.8	0.78	0.81
MFC	-1.14	-1.18	-1.15

4.4 Simultaneous measurement for methanol and ethanol

As it was shown in above sections, both TSCSMF and MFC based sensors display linear wavelength shifts in response to variations of the tested gases concentrations. A key question is whether or not these two sensors working together can be used to simultaneously detect ethanol and methanol. To investigate this it is useful to

develop a second-order matrix showing the relationship between spectral wavelength shifts and gases concentrations as shown by equation (1).

$$\begin{bmatrix} \Delta W_T \\ \Delta W_M \end{bmatrix} = \begin{bmatrix} k_{00} & k_{01} \\ k_{10} & k_{11} \end{bmatrix} \cdot \begin{bmatrix} C_e \\ C_m \end{bmatrix} \quad (1)$$

where ΔW_T and ΔW_M are the wavelength shifts of the TSCSMF and MFC sensors and C_e and C_m correspond to the gas concentrations of ethanol and methanol respectively. The sensor based on TSCSMF has sensitivity coefficients of k_{00} and k_{01} to ethanol and methanol respectively, while for the sensor based on an MFC, the sensitivity coefficients to ethanol and methanol are k_{10} and k_{11} respectively.

From our previous experiments detecting ethanol and methanol separately, the sensitivity values are known to be $k_{00}=0.018$ nm/ppm, $k_{01}=0.005$ nm/ppm, $k_{10}=-0.130$ nm/ppm and $k_{11}=-0.036$ nm/ppm. The ratios $k_{00}/k_{10} = -0.138$ and $k_{01}/k_{11} = -0.139$ are very close, which indicates that these two sensors cannot be used for simultaneous measurement of ethanol and methanol because there would be no unique solution for the matrix. This is most likely because both sensors were coated with materials with the same texture which may show similar absorption properties to the tested VOCs.

To address this problem, a coating mixture prepared with method of recipe II (stirring for a longer time) is employed as a new coating material applied to a new TSCSMF based sample surface. A relatively large tapered waist diameter of $7.0 \mu\text{m}$ is chosen in this case and the fiber surface was coated with a layer formed by 4-pass coating. Due to a longer stirring time applied in the recipe II based coating material, the resulting solution has higher viscosity and higher Nile red concentration, compared to the material prepared in accordance with recipe I. Higher viscosity leads to a thicker coating with larger amount of Nile red, which is confirmed by the SEM image shown in Fig. 6, where a number of large clusters of Nile red particles are observed.

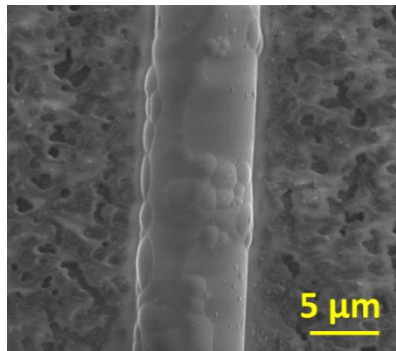


Fig. 6. A SEM images of the new TSCSMF sample after coating with recipe II based material.

Figure 7a shows examples of the measured spectral responses at different ethanol concentrations. The spectral responses for methanol are similar and hence are not shown here for the sake of brevity. Figure 7b summarizes the measured wavelength shift versus different VOCs concentrations, which shows good linearity as well. The measured sensitivities of the new coated TSCSMF sensor are 0.004 nm/ppm to methanol, and 0.007 nm/ppm to ethanol.

When both of the prepared TSCSMF sensors are used, the sensitivity coefficients in the matrix in equation (1) are: $k_{00}=0.018$ nm/ppm, $k_{01}=0.005$ nm/ppm, $k_{10}=0.007$ nm/ppm, $k_{11}=0.004$ nm/ppm. It is clear that the values of $k_{00}/k_{10} = 2.571$ and $k_{01}/k_{11} = 1.25$ are now sufficiently different than the previous case, so that the matrix above can be used for simultaneous measurement of ethanol and methanol concentrations.

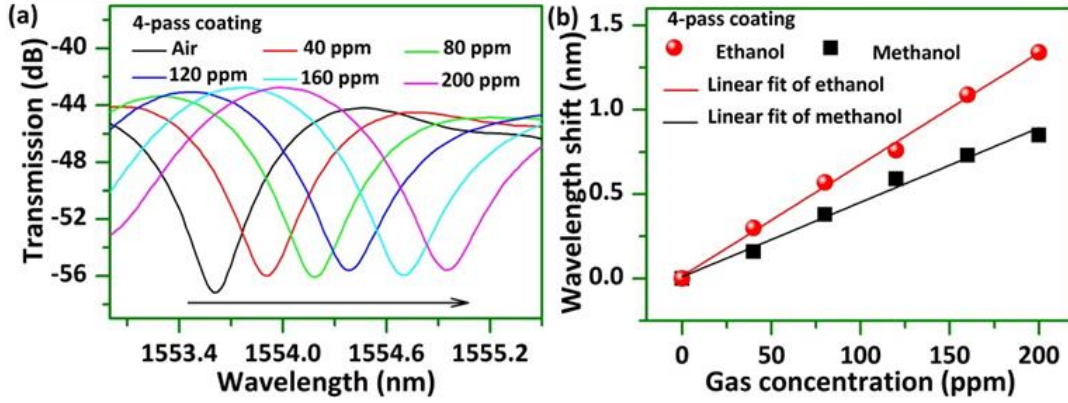


Fig. 7. (a) Normalized measured spectral responses at different concentrations of ethanol for a TSCSMF based 4-pass coating sensor; and (b) corresponding measured wavelength shifts for different VOCs and concentrations.

According to equation (1), the wavelength shifts of the two sensors can be calculated as:

$$\begin{bmatrix} \Delta W_T \\ \Delta W_M \end{bmatrix} = \begin{bmatrix} 0.018 & 0.005 \\ 0.007 & 0.004 \end{bmatrix} \cdot \begin{bmatrix} C_e \\ C_m \end{bmatrix} \quad (2)$$

Solving the matrix for the VOCs concentrations we obtain:

$$\begin{bmatrix} C_e \\ C_m \end{bmatrix} = \begin{bmatrix} 108 & -135 \\ -189 & 486 \end{bmatrix} \cdot \begin{bmatrix} \Delta W_T \\ \Delta W_M \end{bmatrix} \quad (3)$$

As can be seen from the above matrix, by measuring the wavelength shifts for both TSCSMF sensors, two different gases concentrations can be calculated. Using this method, multiple VOCs detection can potentially be realized if a larger number of sensors coated with different recipes are used.

Finally it should be noted that, similar to many other sensors, the proposed sensor suffers from cross sensitivity issues, for example, to temperature, humidity and non-target gases which will introduce measurement errors. However with the technique proposed in this paper, it is possible to use different coating materials to measure the sensors' response to specific influences and then use the commonly report technique to construct a matrix with specific cross-sensitivity coefficients and to realize accurate measurements of the target gases concentrations.

5. Conclusion

In conclusion, TSCSMF and MFC based optical fiber sensors for the detection of methanol and ethanol are proposed and experimentally demonstrated. Coating mixtures of sol-gel silica and Nile red with two different preparation recipes are investigated. Coatings prepared by recipe I were applied to both TSCSMF and MFC samples surfaces. Experimental results show that the sensor based on an MFC shows much better sensitivity of -0.130 nm/ppm to ethanol and -0.036 nm/ppm to methanol than those of the TSCSMF based sensor. The corresponding minimum detectable concentration change are up to 77 ppb and 281 ppb for ethanol and methanol respectively. The response and recovery behaviors in time of the sensors were also investigated. The response time is demonstrated to be less than 5 minutes, while the recovery time varies from 7 minutes to 12 minutes depending on the type of gas and gas concentrations. Both sensors are also proved to have good repeatability of performance. In addition, to investigate the potential for simultaneous measurement of two VOCs, another TSCSMF structure coated with a layer by recipe II was fabricated. A second-order matrix technique was then employed to permit simultaneous measurement of methanol and ethanol concentrations by utilizing both TSCSMF based sensors prepared with different coating recipes.

Acknowledgements

This work was support by FIOSRAIGH 2012 (Dean of Graduate Students' Award); State Key Laboratory of Advanced Optical Communication Systems and Networks, Shanghai Jiao Tong University, China; Science Foundation Ireland (SFI/13/TIDA/B2707, SFI/13/ISCA/2845); the National Natural Science Foundation of China under grant No. 61465009.

References

- [1] K. Demeestere, J. Dewulf, B.D. Witte, H.V. Langenhove, Sample preparation for the analysis of volatile organic compounds in air and water matrices, *J. Chromatogr. A* 1153 (2007) 130–144.
- [2] K. Cherif, J. Mrzacek, S. Hleli, V. Matejec, A. Abdelghani, M. Chomat, N. Jaffrezic-Renault, I. Kasik, Detection of aromatic hydrocarbons in air and water by using xerogel layers coated on PCS fibers excited by an inclined collimated beam, *Sens. Actuators B* 95 (2003) 97–106.
- [3] G. Orellana, D. Haigh, New trends in fiber-optic chemical and biological sensors, *Curr. Anal. Chem.* 4 (2008) 273–295.
- [4] D. Liu, T. Liu, H. Zhang, C. Lv, W. Zeng and J. Zhang, Gas sensing mechanism and properties of Ce-doped SnO₂ sensors, *Mat. Sci. Semicon. Pro.* 15 (2012) 438–444.
- [5] M.J. Fernández, J.L. Fontecha, I. Sayago, M. Aleixandre, J. Lozano, J. Gutiérrez, I. Gracia, C. Cané, and M.C. Horrillo, Discrimination of volatile compounds through an electronic nose based on ZnO SAW sensors, *Sens. Actuators B Chem.* 127 (2007) 277–283.
- [6] B. Li, G. Sauve', M.C. Iovu, M. Jeffries-EL, R. Zhang, J. Cooper, S. Santhanam, L. Schultz, J.C. Revelli, A.G. Kusne, T. Kowalewski, J.L. Snyder, L.E. Weiss, G.K. Fedder, and D.N. Lambeth, Volatile Organic Compound Detection Using Nanostructured Copolymers, *Nano Lett.* 6 (2006) 1598–1602.
- [7] N. A. Rakow, K. S. Suslick, A colorimetric sensor array for odour visualization, *Nature* 460 (2000) 710–713.
- [8] R. Lu, W. Li, B. Mizakoff, A. Katzir, Y. Raichlin, G. Sheng and H. Yu, High-sensitivity infrared attenuated total reflectance sensors for in situ multicomponent detection of volatile organic compounds in water, *Nat. Protoc.* 11 (2016) 377–386.
- [9] M.R.R. Khan, B. Kang, S. Yeom, D. Kwon, S. Kang, Fiber-optic pulse width modulation sensor for low concentration VOC gas, *Sen. Actuators B Chem.* 188 (2013) 689–696.
- [10] C. Elosua, I. Vidondo, F.J. Arregui, C. Barriain, A. Luquin, M. Laguna, I.R. Matias, Lossy mode resonance optical fiber sensor to detect organic vapors, *Sens. Actuators B* 187 (2013) 65–71.
- [11] M.G. Manera, G. Leo, M.L. Curri, P.D. Cozzoli, R. Rella, P. Siciliano, A. Agostiano, L. Vasanelli, Investigation on alcohol vapours/TiO₂ nanocrystal thin films interaction by SPR technique for sensing application, *Sen. Actuators B Chem.* 100 (2004) 75–80.
- [12] A. Dikovska, G. Tanasova, N. Nedyalkov, P. Stefanov, P. Atanasov, E. Karakoleva, A. Andreev, Optical sensing of ammonia using ZnO nanostructure grown on a side-polished optical-fiber, *Sens. Actuators B Chem.* 146 (2010) 331–336.
- [13] S.K. Mishra, D. Kumari, B.D. Gupta, Surface plasmon resonance based fiber optic ammonia gas sensor using ITO and polyaniline, *Sen. Actuators B Chem.* 171–172 (2012), 976–983.
- [14] X. Ning, C. Zhao, F. Shi, S. Jin, Multipoint chemical vapor measurement by zeolite thin film-coated Fresnel reflection-based fiber sensors with an array-waveguide grating, *Sens. Actuators B* 227 (2016) 533–538.
- [15] C. Yu, Y. Wu, C. Li, F. Wu, J. Zhou, Y. Gong, Y. Rao, and Y. Chen, Highly sensitive and selective fiber-optic Fabry-Perot volatile organic compounds sensor based on a PMMA film, *Opt. Mater. Express* 7 (2017) 2111–2116.
- [16] X. Ning, J. Yang, C. Zhao, C. Chan, PDMS-coated fiber volatile organic compounds sensors, *Appl. Opt.* 55 (2016) 3543–3548
- [17] C. Barriain, I. R. Matias, I. Romeo, J. Garrido and M. Laguna, Detection of volatile organic compound vapors by using a vapochromic material on a tapered optical fiber, *Appl. Phys. Lett.* 77 (2000), 2274–2276.
- [18] Y. Chen, C. Lu, Surface modification on silver nanoparticles for enhancing vapor selectivity of localized surface plasmon resonance sensors, *Sen. Actuators B Chem.* 135 (2009) 492–498.
- [19] J. Hromadka, M.C. Partridge, S.W. James, F. Davis, D. Crump, S. Korposh, R. Tatam, Multi-parameter measurements using optical fibre long period gratings for indoor air quality monitoring, *Sens. Actuators B Chem.* 244 (2017) 217–225.
- [20] S. Tao, L. Xu, J. C. Fanguy, Optical fiber ammonia sensing probes using reagent immobilized porous silica coating as transducers, *Sen. Actuators B* 115 (2006) 158–163.
- [21] D. Liu, W. Han, A. K. Mallik, J. Yuan, C. Yu, G. Farrell, Y. Semenova, and Q. Wu, High sensitivity sol-gel silica coated optical fiber sensor for detection of ammonia in water, *Opt. Express* 24 (2016) 24179–24187.
- [22] J.C. Echeverria, M. Faustini, J.J. Garrido, Effects of the porous texture and surface chemistry of silica xerogels on the sensitivity of fiber-optic sensors towards VOCs, *Sens. Actuators B*, 222 (2016) 1166–1174.
- [23] J. Estella, J.C. Echeverria, M. Laguna, J.J. Garrido, Silica xerogels of tailored porosity as support matrix for optical chemical sensors. Simultaneous effect of pH, ethanol:TEOS and water:TEOS molar ratios, and synthesis temperature on gelation time, and textural and structural properties, *J. Non Cryst. Solids* 353 (2007) 286–294.
- [24] J. Estella, J.C. Echeverria, M. Laguna, J.J. Garrido, Effects of aging and drying conditions on the structural and textural properties of silica gels, *Micropor. Mesopor. Mater.* 102 (2007) 274–282.

- [25] D. Liu, A. K. Mallik, J. Yuan, C. Yu, G. Farrell, Y. Semenova, and Q. Wu, High sensitivity refractive index sensor based on a tapered small core single-mode fiber structure, *Opt. Lett.* 40 (2015) 4166–4169.
- [26] L. Sun, Y. Semenova, Q. Wu, D. Liu, J. Yuan, T. Ma, X. Sang, B. Yan, K. Wang, C. Yu, and G. Farrell, High sensitivity ammonia gas sensor based on a silica gel coated microfiber coupler, *IEEE J. Lightwave Technol.* 35 (2017) 2864-2870.
- [27] Q. Wu, Y. Semenova, P. Wang, G. Farrell, A comprehensive analysis verified by experiment of a refractometer based on an SMF28-Small-Core Singlemode fiber (SCSMF) -SMF28 fiber structure, *Journal of Optics*, 13 (2011), 125401.
- [28] A.W. Snyder, Coupled-Mode Theory for Optical Fibers, *J. Opt. Soc. Am.* 62 (1972) 1267-1277.
- [29] C. Reichardt, Solvatochromic dyes as solvent polarity indicators, *Chem. Rev.* 94 (1994) 416-431.
- [30] J.F. Deye, T.A. Berger, A.G. Anderson, Nile red as a solvatochromic dye for measuring solvent strength in normal liquids and mixtures of normal liquids with supercritical and near critical fluids, *Anal. Chem.* 62 (1990) 615-622.
- [31] M.R.R. Khan, S.W. Kang, A high sensitivity and wide dynamic range fiber-optic sensor for low-concentration VOC gas detection, *Sensors*, 14 (2014) 23321-23336.
- [32] M. Kubeckova, M. Sedlar and V. Matejec, Characterization of sol-gel derived coatings on optical fibers, *J. Non-Cryst. Solids* 147&148 (1992) 404-408.